The Journal of Chemical Physics

ABC+D: A time-independent coupled-channel quantum dynamics program for elastic and ro-vibrational inelastic scattering between atoms and triatomic molecules in full dimensionality

Cite as: J. Chem. Phys. **158**, 054801 (2023); https://doi.org/10.1063/5.0137628
Submitted: 04 December 2022 • Accepted: 06 January 2023 • Accepted Manuscript Online: 10 January 2023 • Published Online: 03 February 2023

Dongzheng Yang, Shijie Chai, Daiqian Xie, et al.

The Journal of Chemical Physics ARTICLE scitation.org/journal/jcp

ABC+D: A time-independent coupled-channel quantum dynamics program for elastic and ro-vibrational inelastic scattering between atoms and triatomic molecules in full dimensionality

Cite as: J. Chem. Phys. 158, 054801 (2023); doi: 10.1063/5.0137628
Submitted: 4 December 2022 • Accepted: 6 January 2023 •
Published Online: 3 February 2023

Dongzheng Yang,[1,a] Shijie Chai,[2] Daiqian Xie,[2,3,a] and Hua Guo[1,a]

AFFILIATIONS

[1] Department of Chemistry and Chemical Biology, University of New Mexico, Albuquerque, New Mexico 87131, USA
[2] Institute of Theoretical and Computational Chemistry, School of Chemistry and Chemical Engineering, Nanjing University, Nanjing 210023, China
[3] Hefei National Laboratory, Hefei 230088, China

[a] **Authors to whom correspondence should be addressed:** ydz705@unm.edu; dqxie@nju.edu.cn; and hguo@unm.edu

ABSTRACT

We discuss the details of a time-independent quantum mechanical method and its implementation for full-dimensional non-reactive scattering between a closed-shell triatomic molecule and a closed-shell atom. By solving the time-independent Schrödinger equation within the coupled-channel framework using a log-derivative method, the state-to-state scattering matrix (*S*-matrix) can be determined for inelastic scattering involving both the rotational and vibrational modes of the molecule. Various approximations are also implemented. The ABC+D code provides an important platform for understanding an array of physical phenomena involving collisions between atoms and molecules.

I. INTRODUCTION

Gas phase collisions involving atoms and molecules are responsible for many important physical phenomena, such as reactions and energy transfer.[1] The cross sections and rate coefficients for energy transfer are extensively used in many fields, such as modeling of combustion,[2] interstellar media,[3] and atmospheres.[4] An accurate description of the collision dynamics requires a quantum mechanical treatment because of quantum effects such as discrete internal energy levels, tunneling, and collision resonances. These quantum effects are particularly important and sometimes dominant in cold and ultracold collisions, which have attracted much attention in recent years, thanks to technological advances.[5–11] Significant progress has been made in quantum scattering theory for both non-reactive[12,13] and reactive collisions.[14–21] However, there still exist significant gaps in our ability to describe scattering dynamics. One such case is the full-dimensional treatment of the non-reactive scattering involving polyatomic molecules in cold and ultracold conditions.

At the state-to-state level, scattering is fully described in quantum mechanics by the so-called state-to-state scattering matrix (*S*-matrix),[22] which can be used to compute the experimentally observable differential and integral cross sections. There are two main approaches to computing the *S*-matrix.[15,23] The time-independent (TI) approach solves the time-independent Schrödinger equation using the so-called coupled-channel (CC) approach in which the scattering wavefunction is expanded in terms of a molecular basis. By solving the CC equation along the scattering coordinate with appropriate boundary conditions, elements of the entire *S*-matrix can be extracted. Because of the necessity of matrix inversion, the TI approach scales as N^3, where N is the dimensionality of the system.[24] The alternative is the wave packet (WP) approach, which is based on solving the time-dependent Schrödinger equation[25] or its surrogates.[26–29] The WP approach is

an initial value problem, which scales as N^2, and in favorable cases as $N \log N$, because of the necessary matrix–vector multiplication. As a result, the WP approach is typically more efficient and has been widely used in characterizing quantum reactive and non-reactive scattering.[18,20,21,30] However, the WP approach is difficult to converge at low collision energies due to the long de Broglie wavelength along the scattering coordinate. Consequently, TI is generally considered as the ideal method for treating scattering under cold and ultracold conditions.[8,11]

For non-reactive scattering involving four atoms, there are a few existing software packages. `MOLSCAT`[31] and `HIBRIDON`[32] both work within the rigid rotor approximation, although the former can handle vibrating diatoms. The latter pays special attention to open-shell cases (for extension to vibrating diatoms in atom–diatom scattering see Ref. 33). None is capable of describing vibrationally inelastic scattering involving triatoms. On the other hand, `TwoBC`[34] and our own code (`AB+CD`)[35] are full-dimensional codes but are only applicable to diatom–diatom (2 + 2) scattering. Recently, reduced-dimensional (4D) quantum scattering studies of the ro-vibrational relaxation in the H_2O + He,[36] H_2O + H,[37] and CO_2 + He systems[38] have been reported. However, there has been no full-dimensional TI code for triatom–atom (3 + 1) systems, until recently when we reported the algorithm and applications.[39] In this publication, details of the implementation and information on how to execute the `ABC+D` code are provided.

II. ALGORITHM

A. Coordinates and Hamiltonian

For a triatom-atom system (ABC+D), we choose to work on the coordinates proposed by Brocks, van der Avoird, Sutcliffe, and Tennyson (BAST),[40] depicted in Fig. 1. The z axis of the dimer-fixed (DF) frame is along the inter-monomer vector $\vec{R}$, which is specified by two Euler angles (α, β) with respect to the space-fixed (SF) frame. On the other hand, the orientation of the monomer-fixed (MF) frame attached to monomer ABC is given by three Euler angles $(\alpha_M, \beta_M, \gamma_M)$. Since the potential energy operator (PEO) is independent of α_M, we set $\alpha_M = 0$, $\beta_M \equiv \theta_2$, and $\gamma_M \equiv \phi$, as shown in Fig. 1. The triatomic monomer ABC is described by Radau coordinates $\mathbf{q} \equiv (r_1, r_2, \theta_1)$,[41] which have the advantage that the AB_2 type of triatoms can be treated with proper symmetry adaption. In this coordinate system, the exact kinetic energy operator (KEO) has been worked out,[40] but the expression is not given here due to space limitation.

Atomic units ($\hbar = 1$) are assumed throughout the manuscript as well as in the `ABC+D` code unless specifically pointed out. Here, we ignore the electronic and spin quantum numbers in both collision partners. The total nuclear Hamiltonian for scattering between ABC and D is written as

$$\hat{H} = -\frac{1}{2\mu}\frac{\partial^2}{\partial R^2} + \frac{(\mathbf{J} - \mathbf{j}_2)^2}{2\mu R^2} + \hat{h}_{\mathrm{ABC}}(\mathbf{j}_2, \mathbf{q}) + \Delta V(R, r_1, r_2, \theta_1, \theta_2, \phi) \tag{1}$$

in which $\mu \equiv \frac{m_{\mathrm{ABC}} m_{\mathrm{D}}}{m_{\mathrm{ABC}} + m_{\mathrm{D}}}$ is the reduced mass between the two collision partners and $\Delta V(R, r_1, r_2, \theta_1, \theta_2, \phi) \equiv V_{\mathrm{tot}}(R, r_1, r_2, \theta_1, \theta_2, \phi) - V_{\mathrm{ABC}}(r_1, r_2, \theta_1)$ is the interaction PEO, where V_{tot} is the total PEO of the ABC+D system and V_{ABC} is that of monomer ABC. Here, $\mathbf{j}_2$ is the rotational angular momentum of ABC, which is coupled with the orbital angular momentum $\mathbf{L}$ to yield the total angular momentum $\mathbf{J} = \mathbf{j}_2 + \mathbf{L}$. The Hamiltonian of monomer ABC is

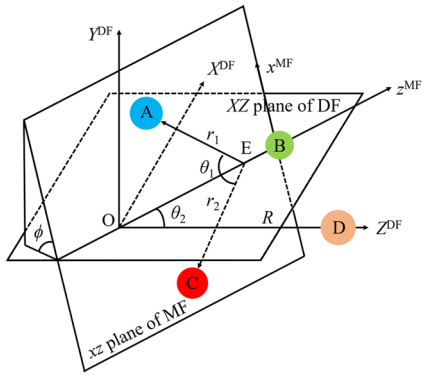

FIG. 1. The BAST coordinates $(R, r_1, r_2, \theta_1, \theta_2, \phi)$. (X^{DF}, Y^{DF}, Z^{DF}) labels the axes of DF frame, while (x^{MF}, y^{MF}, z^{MF}) labels the MF frame. Note that z^{MF} is along $\overrightarrow{EB}$ and y^{MF} is along $\vec{r}_1 \times \vec{r}_2$. The origin O is the center of mass of monomer ABC and E is the Radau canonical point of monomer ABC. $\overrightarrow{EB}$ is the cross line of XZ plane of the DF frame and the xz plane of the MF frame.

$$\hat{h}_{\mathrm{ABC}} = \hat{h}_1 + \hat{h}_2 + \hat{T}_{\mathrm{vr}} + V_{\mathrm{res}}, \tag{2}$$

where the one-dimensional (1D) reference Hamiltonians are

$$\begin{aligned} \hat{h}_1(r_1) &= -\frac{1}{2m_{\mathrm{A}}}\frac{\partial^2}{\partial r_1^2} + V_1(r_1), \\ \hat{h}_2(r_2) &= -\frac{1}{2m_{\mathrm{C}}}\frac{\partial^2}{\partial r_2^2} + V_2(r_2). \end{aligned} \tag{3}$$

The 1D reference PEOs are obtained from V_{ABC}, with other degrees of freedom fixed at, for example, equilibrium,

$$\begin{aligned} V_1(r_1) &= V_{\mathrm{ABC}}(r_1, r_2 = r_{2,\mathrm{eq}}, \theta_1 = \theta_{1,\mathrm{eq}}), \\ V_2(r_2) &= V_{\mathrm{ABC}}(r_1 = r_{1,\mathrm{eq}}, r_2, \theta_1 = \theta_{1,\mathrm{eq}}). \end{aligned} \tag{4}$$

The residual PEO is thus defined as $V_{\mathrm{res}}(r_1, r_2, \theta_1) = V_{\mathrm{ABC}}(r_1, r_2, \theta_1) - V_1(r_1) - V_2(r_2)$. The ro-vibrational KEO $\hat{T}_{\mathrm{vr}}$ for a triatomic molecule in the Radau coordinates can be found in Ref. 42, so not given here.

B. Coupled-channel equations

In the time-independent coupled-channel (TICC) approach, the scattering wavefunction is expanded in terms of a basis set and the time-independent Schrödinger equation is solved numerically by propagating on a grid along the R coordinate, using, for example, the log-derivative (LogD) method.[43,44] Unlike the diatom–diatom case where the ro-vibrational states of the diatoms represent a natural choice, the optimal selection of the basis functions in the atom–triatom collision is the key to render the calculations efficient.

We choose to implement the CC approach for non-reactive scattering between ABC and D by expanding the total scattering wavefunction in terms of the eigenfunctions of $\hat{h}_{\mathrm{ABC}}$, or the contracted basis,

$$\Psi^{JM\varepsilon} = \sum_{\eta} F_{\eta}^{J\varepsilon}(R)|\eta; JM\varepsilon\rangle, \tag{5}$$

where $\eta \equiv (j_2 tK)$ is the collective index for an asymptotic channel and t is defined below. The contracted basis satisfies $\hat{h}_{\mathrm{ABC}}|\eta; JM\varepsilon\rangle = E_{\mathrm{int},\eta}|\eta; JM\varepsilon\rangle$, with $E_{\mathrm{int},\eta}$ as the internal energy of the ηth channel. Substituting Eqs. (1) and (5) into the time-independent Schrödinger equation leads to the CC equations

$$\left(\frac{\mathrm{d}^2}{\mathrm{d}R^2} + k_{\eta}^2\right) F_{\eta}^{J\varepsilon} = \sum_{\eta'} \left(2\mu V_{\eta',\eta}^{J\varepsilon} + \frac{1}{R^2} U_{\eta',\eta}^{J\varepsilon}\right) F_{\eta'}^{J\varepsilon}. \tag{6}$$

Here, the channel wave vector $k_{\eta}^2 = 2\mu E_{\mathrm{c},\eta}$ is defined with the corresponding collision energy $E_{\mathrm{c},\eta} = E - E_{\mathrm{int},\eta}$, where E is the total energy. The construction of the basis, the evaluation of the centrifugal matrix $\mathbf{U}$ and interaction potential matrix $\mathbf{V}$, and the numerical solution of the CC equations using the LogD method are discussed below.

C. Primitive basis

We first define an unsymmetrized primitive basis set in a direct product form, from which all basis functions are assembled. For the angular part, it is given in an uncoupled form

$$|j_1\Omega j_2 K; JM\rangle \equiv |JMK\rangle |j_2 K\Omega\rangle |j_1\Omega\rangle, \tag{7}$$

where

$$\begin{aligned} \langle \alpha, \beta, 0|JMK\rangle &\equiv \sqrt{\frac{2J+1}{4\pi}} D_{M,K}^{J*}(\alpha, \beta, 0), \\ \langle 0, \theta_2, \phi|j_2 K\Omega\rangle &\equiv \sqrt{\frac{2J+1}{4\pi}} D_{K,\Omega}^{j_2*}(0, \theta_2, \phi), \\ \langle \theta_1|j_1\Omega\rangle &\equiv \Theta_{j_1}^{\Omega}(\theta_1). \end{aligned} \tag{8}$$

Here, $D_{M,K}^{J}$ is a Wigner rotational matrix element, and $\Theta_{j_1}^{\Omega}$ is a normalized associated Legendre function.[45] $\mathbf{j}_1$ is the rotational angular momentum corresponding to θ_1, which along with $\mathbf{j}_2$ has the MF z axis projection as Ω. The projection of $\mathbf{J}$ onto the SF z axis is given by M, which along with $\mathbf{j}_2$ has the projection onto the DF z axis as K.

As monomer ABC does not undergo bond breaking during non-reactive scattering, an optimized basis can be designed. To this end, the eigenfunctions of the 1D reference Hamiltonians, *i.e.*,

$$\begin{aligned} \hat{h}_1|v_1\rangle &= E_{1,v_1}|v_1\rangle, \\ \hat{h}_2|v_2\rangle &= E_{2,v_2}|v_2\rangle, \end{aligned} \tag{9}$$

were solved using the sine discrete variable representation (sine-DVR),[46] in which

$$\begin{aligned} \langle r_1|n_1\rangle &\equiv \sqrt{\frac{2}{b_1 - a_1}} \sin\frac{n_1\pi(r_1 - a_1)}{b_1 - a_1}, \\ \langle r_2|n_2\rangle &\equiv \sqrt{\frac{2}{b_2 - a_2}} \sin\frac{n_2\pi(r_2 - a_2)}{b_2 - a_2}, \end{aligned} \tag{10}$$

where a and b define the ranges over r. The sine-DVR grid points labeled by l_1 and l_2 are given as $r_{1,l_1} = a_1 + \frac{l_1(b_1 - a_1)}{M_1 + 1}$ and $r_{2,l_2} = a_2 + \frac{l_2(b_2 - a_2)}{M_2 + 1}$, where M_1 and M_2 are the total numbers of DVR points (also the numbers of bases $|n_1\rangle$ and $|n_2\rangle$, respectively). The 1D reference Hamiltonian matrices in DVR are constructed as

$$\begin{aligned} \left\langle l_1'\middle|\hat{h}_1\middle|l_1\right\rangle &= \tilde{K}_{l_1',l_1} + \delta_{l_1',l_1} V_1(r_{1,l_1}), \\ \left\langle l_2'\middle|\hat{h}_2\middle|l_2\right\rangle &= \tilde{K}_{l_2',l_2} + \delta_{l_2',l_2} V_2(r_{2,l_2}), \end{aligned} \tag{11}$$

where the sine-DVR kinetic energy matrices $\tilde{K}$ are evaluated analytically according to Ref. 46, while the potential energy matrices are diagonal in DVR. By diagonalizing the 1D reference Hamiltonian matrices, the eigenvalues E_1 and E_2 and the corresponding orthogonal eigenvectors $\xi_{l_1 v_1}$ and $\zeta_{l_2 v_2}$ are obtained, where

$$\begin{aligned} |v_1\rangle &= \sum_{l_1} \xi_{l_1 v_1} |l_1\rangle, \\ |v_2\rangle &= \sum_{l_2} \zeta_{l_2 v_2} |l_2\rangle. \end{aligned} \tag{12}$$

To further improve the efficiency, the potential-optimized DVR (PODVR)[47,48] can be used. The corresponding PODVR grids, denoted as r_{1,p_1} and r_{2,p_2}, are given by the eigenvalues of the $\langle v_1'|r_1|v_1\rangle = \sum_{l_1} \xi_{l_1 v_1'} \xi_{l_1 v_1} r_{1,l_1}$ and $\langle v_2'|r_2|v_2\rangle = \sum_{l_2} \zeta_{l_2 v_2'} \zeta_{l_2 v_2} r_{2,l_2}$ matrices, respectively. The corresponding eigenvectors $\rho_{v_1 p_1}$ and $\tau_{v_2 p_2}$ can then be used in evaluating the reference Hamiltonians, $\left\langle p_1'\middle|\hat{h}_1\middle|p_1\right\rangle = \sum_{v_1} \rho_{v_1 p_1'} \rho_{v_1 p_1} E_{1,v_1}$ and $\left\langle p_2'\middle|\hat{h}_2\middle|p_2\right\rangle = \sum_{v_2} \tau_{v_2 p_2'} \tau_{v_2 p_2} E_{2,v_2}$, respectively. The transformation matrices between the PODVR and the finite basis representation (FBR), namely $P_{p_1 v_1}$ and $Q_{p_2 v_2}$, are obtained by diagonalizing the above Hamiltonian matrices, and they are used in calculating the quadrature below. In practice, DVR basis $|l_1\rangle$ and $|l_2\rangle$ are chosen to construct the 1D reference Hamiltonian matrices in Eq. (11). While the number of DVR points could be a few hundred, only several eigenfunctions $|v_1\rangle$ and $|v_2\rangle$ are stored for later use, and the choice of the maximum numbers of them, $v_{1\max}$ and $v_{2\max}$, corresponds to $v_{1\max} + 1$ and $v_{2\max} + 1$ PODVR points, respectively.

Then, the parity-adapted (PA) primitive basis set is defined in terms of a direct product of unsymmetrized primitive basis functions

$$|j_1\Omega v_1 v_2 j_2 K; JM\varepsilon\rangle = |v_1 v_2\rangle |j_1\Omega j_2 K; JM\varepsilon\rangle, \tag{13}$$

where the PA angular basis is

$$\begin{aligned} |j_1\Omega j_2 K; JM\varepsilon\rangle = \frac{1}{\sqrt{2 + 2\delta_{K0}\delta_{\Omega 0}}} \big[&|j_1\Omega j_2 K; JM\rangle \\ &+ \varepsilon(-1)^J |j_1(-\Omega) j_2(-K); JM\rangle \big]. \end{aligned} \tag{14}$$

The PA radial basis depends on the symmetry of ABC. If A and C are identical (an A_2B type triatom), we have

$$\langle r_1, r_2|v_1 v_2\rangle = \frac{1}{\sqrt{2 + 2\delta_{v_1 v_2}}} \big[\langle r_1|v_1\rangle\langle r_2|v_2\rangle + p_v \langle r_2|v_1\rangle\langle r_1|v_2\rangle\big], \tag{15}$$

where p_v is defined below. Otherwise, we have

$$\langle r_1, r_2|v_1 v_2\rangle = \langle r_1|v_1\rangle\langle r_2|v_2\rangle. \tag{16}$$

The PA primitive basis functions are eigenfunctions of the space inversion parity ε (corresponding to the operator $\hat{E}^*$),

$$\hat{E}^*|j_1\Omega v_1 v_2 j_2 K; JM\varepsilon\rangle = \varepsilon|j_1\Omega v_1 v_2 j_2 K; JM\varepsilon\rangle. \tag{17}$$

For A_2B type triatoms, an additional symmetry, nuclear exchange parity P_{ex}, is added,

$$\hat{P}_{ex}|j_1\Omega v_1 v_2 j_2 K; JM\varepsilon\rangle = p_v(-1)^{\Omega}|j_1\Omega v_1 v_2 j_2 K; JM\varepsilon\rangle. \tag{18}$$

In practice, ε and $P_{ex} = p_v(-1)^{\Omega}$ are, respectively, set to be either +1 or −1 as conserved quantities in the calculation. In the PA basis, the quantum numbers K and Ω are restricted because the combination of unsymmetrized functions renders some terms of PA functions to vanish. For both even and odd total parities $p \equiv \varepsilon(-1)^J = \pm 1$, the restrictions are (i) $K \geq 0$ and (ii) for $K = 0$, Ω is restricted to non-negative integers. We note that $j_2 \neq 0$ for odd total parity $p = -1$, and $K = \Omega = 0$ only exists for even total parity $p = +1$. For A_2B-type triatoms with exchange symmetry, there are additional restrictions: (i) $v_1 \geq v_2$ and (ii) for $v_1 = v_2$, only the $p_v = 1$ terms survive. On the other hand, there is no restriction on v_1 and v_2 for ABC-type triatoms.

In scattering calculations, the rovibrational eigenfunctions of monomer ABC $|\eta; JM\varepsilon\rangle$ serve as the contracted basis to reduce the size of the Log D matrix. To this end, the contracted and PA primitive bases are related by a transformation matrix $\mathbf{T}$,

$$|j_2 tK; JM\varepsilon\rangle = \sum_{\chi} T^{j_2 K}_{\chi' t}|\chi j_2 K; JM\varepsilon\rangle, \tag{19}$$

where $\chi \equiv (j_1\Omega v_1 v_2)$ is the collective index of the primitive basis and t labels a ro-vibrational internal state of monomer ABC. The $\mathbf{T}$ matrix is obtained by diagonalizing the monomer's Hamiltonian matrix in the PA primitive basis. In principle, the Hamiltonian matrix elements can be evaluated directly in terms of PA basis functions, but we find the equations are tedious and complex (albeit analytical), due to the combination over $\pm K$ and $\pm\Omega$ in Eq. (14). In the `ABC+D` program, our strategy is to first evaluate the Hamiltonian matrix elements in the unsymmetrized basis, $\left\langle \chi' j_2 K\middle|\hat{h}_{ABC}\middle|\chi j_2 K\right\rangle$ and then transform it into the PA basis, $\left\langle \chi' j_2 K; JM\varepsilon\middle|\hat{h}_{ABC}\middle|\chi j_2 K; JM\varepsilon\right\rangle$. The nonzero elements of the KEO in the unsymmetrized basis have been reported by Wang and Carrington[42] and is given as follows:

$$\begin{aligned}
\left\langle \chi j_2 K\middle|\hat{h}_1 + \hat{h}_2\middle|\chi j_2 K\right\rangle &= E_{1,v_1} + E_{2,v_2},\\
\left\langle j_1'\Omega v_1' v_2' j_2 K\middle|\hat{T}_{vr}\middle|j_1\Omega v_1 v_2 j_2 K\right\rangle &= (\delta_{v_2',v_2}B_{v_1'v_1} + \delta_{v_1',v_1}C_{v_2'v_2})\\
&\quad\times\left\{\frac{1}{8}\delta_{j_1',j_1}\left[j_2(j_2+1)-\Omega^2\right] + \delta_{j_1',j_1}j_1(j_1+1) + \frac{1}{4}\left[j_2(j_2+1)-3\Omega^2\right]E_{j_1',j_1\Omega}\right\},\\
\left\langle j_1'(\Omega\pm 1)v_1' v_2' j_2 K\middle|\hat{T}_{vr}\middle|j_1\Omega v_1 v_2 j_2 K\right\rangle &= \frac{1}{4}(\delta_{v_2',v_2}B_{v_1'v_1} - \delta_{v_1',v_1}C_{v_2'v_2})\lambda^{\pm}_{j_2\Omega}\left[(2\Omega\pm 1)\left(G^{\pm}_{j_1',j_1\Omega} - D^{\pm}_{j_1',j_1\Omega}\right) - 2\delta_{j_1',j_1}\lambda^{\pm}_{j_1\Omega}\right],\\
\left\langle j_1'(\Omega\pm 2)v_1' v_2' j_2 K\middle|\hat{T}_{vr}\middle|j_1\Omega v_1 v_2 j_2 K\right\rangle &= \frac{1}{16}(\delta_{v_2',v_2}B_{v_1'v_1} + \delta_{v_1',v_1}C_{v_2'v_2})\lambda^{\pm}_{j_2\Omega}\lambda^{\pm}_{j_2(\Omega\pm1)}\left(2F^{\pm}_{j_1',j_1\Omega} - H^{\pm}_{j_1',j_1\Omega}\right),
\end{aligned} \tag{20}$$

where $\lambda^{\pm}_{ab} = \sqrt{a(a+1) - b(b\pm 1)}$. Matrices $\mathbf{B}$, $\mathbf{C}$, $\mathbf{D}$, $\mathbf{F}$, $\mathbf{G}$, and the residual PEO matrix elements $\left\langle \chi' j_2 K\middle|V_{res}\middle|\chi j_2 K\right\rangle$ are discussed below.

For simplicity, we drop irrelevant quantum numbers and the operator $\hat{h}_{ABC}$ in the middle of the Dirac bracket in Eqs. (21) and (22). For ABC triatoms without exchange symmetry, PA matrix elements need be calculated only for $K = 0$ block,

$$\begin{aligned}
\langle\Omega'|\Omega\rangle^{K=0,\varepsilon} &= \frac{1}{\sqrt{2+2\delta_{\Omega',0}}}\frac{1}{\sqrt{2+2\delta_{\Omega,0}}}\left[\langle\Omega'|\Omega\rangle + \varepsilon(-1)^J\right.\\
&\quad\left.\times\left(\langle -\Omega'|\Omega\rangle + \langle\Omega'|-\Omega\rangle\right) + \langle -\Omega'|-\Omega\rangle\right]\\
&= \frac{1}{\sqrt{1+\delta_{\Omega',0}}}\frac{1}{\sqrt{1+\delta_{\Omega,0}}}\left[\langle\Omega'|\Omega\rangle + \varepsilon(-1)^J\langle -\Omega'|\Omega\rangle\right].
\end{aligned} \tag{21}$$

This is because that for $K > 0$, the unrestricted quantum numbers of PA basis functions are identical to those of the unsymmetrized one and that the cross terms for K and $-K$ equal to zero. Otherwise for A_2B-type triatoms, an additional combination of matrix elements dependent on v_1 and v_2 is carried out for all K blocks,

$$\begin{aligned}
\langle v_1' v_2'|v_1 v_2\rangle^{P_{ex}} &= \frac{1}{\sqrt{2+2\delta_{v_1',v_2'}}}\frac{1}{\sqrt{2+2\delta_{v_1,v_2}}}\\
&\quad\times\left[\langle v_1' v_2'|v_1 v_2\rangle + p'_v\langle v_2' v_1'|v_1 v_2\rangle\right.\\
&\quad\left.+ p_v\langle v_1' v_2'|v_2 v_1\rangle + p'_v p_v\langle v_2' v_1'|v_2 v_1\rangle\right].
\end{aligned} \tag{22}$$

In summary, the diagonalization is carried out individually for each j_2, K-labeled triatomic Hamiltonian matrix block. For the $K = 0$ block, the diagonalization is obviously needed. For matrix blocks labeled by positively valued K, the eigenvalues E_{int} and the transformation matrix $\mathbf{T}$ are obtained by diagonalizing the matrix

only once ($K = 1$ in the ABC+D program). We emphasize that although a large number of primitive basis $|\chi\rangle$ may be involved in Eq. (19), only a few specifically selected contracted basis $|\eta\rangle$ need be included in the CC equations [Eq. (5)]. The use of this contracted basis significantly reduces the size of the matrices needed in CC equations. In the ABC+D program, we also provide an optional choice of using a customized contracted basis consisting of only desired $(j_2 t)$ pairs. We also note that a triatomic molecule can be either linear rotor or a symmetric and asymmetric top so that different labels of ro-vibrational states are needed. Nonetheless, the quantum numbers $(j_2 t)$ pairs used here are general for all types of triatomic molecules.

D. Evaluation of matrix elements

The residual potential matrix is expressed explicitly as

$$\begin{aligned}\langle \chi' j_2 K | V_{\rm res} | \chi j_2 K \rangle &\equiv \delta_{\Omega',\Omega} \langle v'_1 v'_2 | \langle j'_1 \Omega | V_{\rm res}(r_1, r_2, \theta_1) | j_1 \Omega \rangle | v_1 v_2 \rangle \\ &= \delta_{\Omega',\Omega} \sum_{p_1 p_2 p_3} P_{p_1 v'_1} P_{p_1 v_1} Q_{p_2 v'_2} \\ &\quad \times Q_{p_2 v_2} w_{p_3} \Theta^{\Omega}_{j'_1} \Theta^{\Omega}_{j_1} V_{\rm res}(r_{1,p_1}, r_{2,p_2}, \theta_{1,p_3}), \end{aligned} \tag{23}$$

where w_{p_3} is the weighting factor of the corresponding Gauss–Legendre quadrature of θ_1. The quadrature is calculated directly without any intermediate matrices.

The matrices **B**, **C**, **D**, **F**, and **G** are expressed as

$$\begin{aligned} B_{v'_1 v_1} &= \frac{1}{2m_{\rm A}} \left\langle v'_1 \left| \frac{1}{r_1^2} \right| v_1 \right\rangle = \frac{1}{2m_{\rm A}} \sum_{p_1} P_{p_1 v'_1} P_{p_1 v_1} \frac{1}{r_1^2}, \\ C_{v'_2 v_2} &= \frac{1}{2m_{\rm C}} \left\langle v'_2 \left| \frac{1}{r_2^2} \right| v_2 \right\rangle = \frac{1}{2m_{\rm C}} \sum_{p_2} Q_{p_2 v'_2} Q_{p_2 v_2} \frac{1}{r_2^2}, \\ D^{\pm}_{j'_1 j_1 \Omega} &= \left\langle \Theta^{\Omega \pm 1}_{j'_1} | \cot\ \theta_1 \left| \Theta^{\Omega}_{j_1} \right\rangle = \sum_{p_3} w_{p_3} \Theta^{\Omega \pm 1}_{j'_1}(\theta_{1,p_3}) \Theta^{\Omega}_{j_1}(\theta_{1,p_3}) \cot\ \theta_{1,p_3}, \right. \\ E_{j'_1 j_1 \Omega} &= \left\langle \Theta^{\Omega}_{j'_1} \left| \frac{1}{1+\cos\theta_1} \right| \Theta^{\Omega}_{j_1} \right\rangle = \sum_{p_3} w_{p_3} \Theta^{\Omega}_{j'_1}(\theta_{1,p_3}) \Theta^{\Omega}_{j_1}(\theta_{1,p_3}) \frac{1}{1+\cos\ \theta_{1,p_3}}, \\ F^{\pm}_{j'_1 j_1 \Omega} &= \left\langle \Theta^{\Omega \pm 2}_{j'_1} \left| \frac{1}{1+\cos\ \theta_1} \right| \Theta^{\Omega}_{j_1} \right\rangle = \sum_{p_3} w_{p_3} \Theta^{\Omega \pm 2}_{j'_1}(\theta_{1,p_3}) \Theta^{\Omega}_{j_1}(\theta_{1,p_3}) \frac{1}{1+\cos\ \theta_{1,p_3}}, \\ G^{\pm}_{j'_1 j_1 \Omega} &= \left\langle \Theta^{\Omega \pm 1}_{j'_1} \left| \frac{1}{\sin\ \theta_1} \right| \Theta^{\Omega}_{j_1} \right\rangle = \sum_{p_3} w_{p_3} \Theta^{\Omega \pm 1}_{j'_1}(\theta_{1,p_3}) \Theta^{\Omega}_{j_1}(\theta_{1,p_3}) \frac{1}{\sin\theta_{1,p_3}}, \\ H^{\pm}_{j'_1 j_1 \Omega} &= \left\langle \Theta^{\Omega \pm 2}_{j'_1} \right| \left. \Theta^{\Omega}_{j_1} \right\rangle = \sum_{p_3} w_{p_3} \Theta^{\Omega \pm 2}_{j'_1}(\theta_{1,p_3}) \Theta^{\Omega}_{j_1}(\theta_{1,p_3}), \end{aligned} \tag{24}$$

in which matrices **B** and **C** are calculated by PODVR, and matrices **E**, **F**, **G**, and **H** are evaluated by a Gauss–Legendre quadrature over θ_1.

The centrifugal matrix **U** is analytical as given,

$$\begin{aligned} U_{\eta',\eta} &\equiv \langle \eta' | (\mathbf{J} - \mathbf{j}_2)^2 | \eta \rangle \\ &= \delta_{t',t} \delta_{j'_2, j_2} \left\{ \delta_{K',K} \left[J(J+1) + j_2(j_2+1) - 2K^2 \right] \right. \\ &\quad \left. - \delta_{K',K+1} \sqrt{1+\delta_{K0}} \lambda^{+}_{JK} \lambda^{+}_{j_2 K} - \delta_{K',K-1} \sqrt{1+\delta_{K1}} \lambda^{-}_{JK} \lambda^{-}_{j_2 K} \right\}. \end{aligned} \tag{25}$$

The interaction PEO matrix is

$$V_{\eta',\eta} \equiv \delta_{K',K} \langle j'_2 t' K | \Delta V | j_2 t K \rangle. \tag{26}$$

The calculation of **V** is carried out by firstly evaluating the values of the real and imaginary parts of the contracted basis $|j_2 t K\rangle$ at each quadrature point using Eq. (19). Written explicitly,

$$\begin{aligned} \text{real}\left[|j_2 t K\rangle_{p_1 p_2 l_3 l_4 l_5} \right] &= \sum_{\chi} T^{j_2 K}_{\chi t} \Phi_{v_1 v_2}(r_{1,p_1}, r_{2,p_2}) \Theta^{\Omega}_{j_1} \\ &\quad \times (\theta_{1,l_3}) \bar{d}^{j_2}_{K,\Omega}(\theta_{2,l_4}) \cos(\Omega \phi_{l_5}), \\ \text{imag}\left[|j_2 t K\rangle_{p_1 p_2 l_3 l_4 l_5} \right] &= \sum_{\chi} T^{j_2 K}_{\chi t} \Phi_{v_1 v_2}(r_{1,p_1}, r_{2,p_2}) \Theta^{\Omega}_{j_1} \\ &\quad \times (\theta_{1,l_3}) \bar{d}^{j_2}_{K,\Omega}(\theta_{2,l_4}) \sin(\Omega \phi_{l_5}), \end{aligned} \tag{27}$$

where $\bar{d}^{j_2}_{K,\Omega} \equiv \sqrt{\frac{2j_2+1}{2}} d^{j_2}_{K,\Omega}$ is a normalized reduced Wigner rotational function.[45] In ABC+D, the values of contracted basis are evaluated in terms of intermediate matrices as follows:

$$\begin{aligned} IMA_{j_2 t K \Omega v_1 v_2, l_3 l_4} &= RTF_{j_2 K \Omega l_4} \sum_{j_1} T^{j_2 K}_{j_1 \Omega v_1 v_2 t} ALP_{j_1 \Omega l_3}, \\ IMB_{j_2 t K \Omega, p_1 p_2 l_3 l_4} &= \sum_{v_1 v_2} IMA_{j_2 t K \Omega v_1 v_2, l_3 l_4} RDF_{v_1 v_2 p_1 p_2}, \\ \text{real}\left[|j_2 t K\rangle_{p_1 p_2 l_3 l_4 l_5} \right] &= \sum_{\Omega} w_{l_5} \cos(\Omega \phi_{l_5}) IMB_{j_2 t K \Omega, p_1 p_2 l_3 l_4}, \\ \text{imag}\left[|j_2 t K\rangle_{p_1 p_2 l_3 l_4 l_5} \right] &= \sum_{\Omega} w_{l_5} \sin(\Omega \phi_{l_5}) IMB_{j_2 t K \Omega, p_1 p_2 l_3 l_4}, \end{aligned} \tag{28}$$

where the various intermediate matrices are given as follows with their corresponding Gauss-Legendre quadrature weight factors w_l:

$$\begin{aligned} ALP_{j_1\Omega l_3} &= \sqrt{w_{l_3}}\Theta^{\Omega}_{j_1}(\cos\,\theta_{1,l_3}),\\ RTF_{j_2K\Omega l_4} &= \sqrt{w_{l_4}}\bar{d}^{j_2}_{K,\Omega}(\theta_{2,l_4}),\\ IPS^{l_R}_{p_1p_2l_3l_4l_5} &= \Delta V(R_{l_R}, r_{1,p_1}, r_{2,p_2}, \theta_{1,l_3}, \theta_{2,l_4}, \phi_{l_5}). \end{aligned} \tag{29}$$

For the ABC-type monomer,

$$RDF_{v_1v_2p_1p_2} = P_{p_1v_1}Q_{p_2v_2}; \tag{30}$$

otherwise, for the A_2B-type monomer,

$$RDF^{p_v}_{v_1v_2p_1p_2} = \frac{1}{\sqrt{2+2\delta_{v_1,v_2}}}(P_{p_1v_1}Q_{p_2v_2} + p_vP_{p_1v_2}Q_{p_2v_1}). \tag{31}$$

Then, the interaction PEO matrix as a function of intermolecular distance R is evaluated by summing over all quadrature grid points,

$$\begin{aligned} &\langle j_2' t' K'|\Delta V|j_2 tK\rangle^{l_R}\\ &= \frac{1}{\pi}\delta_{K',K}\sum_{p_1p_2l_3l_4l_5}\Big(\mathrm{real}\Big[\langle j_2' t' K\rangle_{p_1p_2l_3l_4l_5}\Big]\mathrm{real}\Big[\langle j_2 tK\rangle_{p_1p_2l_3l_4l_5}\Big]\\ &\quad + \mathrm{imag}\Big[\langle j_2' t' K\rangle_{p_1p_2l_3l_4l_5}\Big]\mathrm{imag}\Big[\langle j_2 tK\rangle_{p_1p_2l_3l_4l_5}\Big]\Big)IPS^{l_R}_{p_1p_2l_3l_4l_5}. \end{aligned} \tag{32}$$

This fivefold summation represents the most time-demanding computational task in the ABC+D program. Luckily, the **V** matrix is independent of total energy E, which allows calculations of the S-matrix at several total energies in a single run, by storing the same **V** matrix in the virtual memory.

Furthermore, we note that a direct claim of arrays/matrices in terms of indices may cause difficulties in flipping over of storage reading pointer because of the high dimensionality of these intermediate matrices. Indeed, FORTRAN77 compilers allow at most a seven-dimensional claim of an array. To realize the vectorization of these matrices, integer arrays that record the correspondence relationship between the sequential number (collective index) and each index is prepared initially and used to facilitate the definition of one-dimensional arrays with composite indices.

E. Propagation of log-derivative matrix and extraction of *S*-matrix

We follow closely Manolopoulos' potential-following improved LogD method[44] and apply it in ABC+D. A brief introduction of the algorithm is given here. The CC equations [Eq. (6)] can be rewritten in the following form:

$$\frac{\mathrm{d}^2F_\eta(R)}{\mathrm{d}R^2} = \mathbf{W}(R)F_\eta(R), \tag{33}$$

where the coupled matrix **W** is

$$W_{\eta',\eta}(R) = \frac{U_{\eta',\eta}}{R^2} + 2\mu V_{\eta',\eta}(R) - \delta_{\eta',\eta}k^2_\eta. \tag{34}$$

By defining the log-derivative matrix $\mathbf{Y} \equiv \frac{\mathrm{d}\mathbf{F}}{\mathrm{d}R}\mathbf{F}^{-1}$, the second-order differential equation [Eq. (33)] can be converted to a first-order differential equation (or the so-called Riccati equation),

$$\frac{\mathrm{d}\mathbf{Y}}{\mathrm{d}R} = \mathbf{W} - \mathbf{Y}^2. \tag{35}$$

In principle, the particular solution of a first-order differential equation can be obtained by assigning only one boundary condition. As for non-reactive scattering problems, the boundary condition is straightforward: at the classical forbidden radius $R = R_0$, where the potential energy is much larger than the total energy and the scattering wavefunction vanishes, $F_\eta(R_0) = 0$. This leads the initial logD matrix $\mathbf{Y}(R_0) = \infty\mathbf{I}$, where **I** is the identity matrix. Alternatively, the Wentzel–Kramers–Brillouin (WKB) boundary condition[49] is applied,

$$Y_{\eta',\eta}(R_0) = \delta_{\eta',\eta}\big[W_{\eta',\eta}(R_0)\big]^{1/2}, \tag{36}$$

which typically converges faster.

We note in passing that the capture calculations can be used in statistical quantum modeling of scattering.[50,51] Such a statistical model is quite useful in characterizing quantum scattering via a long-lived intermediate.[19,52] The capture boundary condition implemented in our AB+CD code[53] has been applied successfully in the ultracold KRb + KRb → K_2 + Rb_2 calculations.[54] For capture scattering problems, the WKB initial boundary condition is set as an imaginary absorption potential at $R = R_c$,

$$Y_{\eta',\eta}(R_c) = \delta_{\eta',\eta}\begin{cases} -\mathrm{i}\sqrt{-W_{\eta,\eta}(R_c)} & [W_{\eta,\eta}(R_c) \le 0],\\ \sqrt{W_{\eta,\eta}(R_c)} & [W_{\eta,\eta}(R_c) > 0]. \end{cases} \tag{37}$$

Although we do not provide such an option in the ABC+D program, it is straightforward to extend the current version to study capture scattering problems using Eq. (37).

With the appropriate initial LogD matrix, $\mathbf{Y}(R_0)$ is propagated to the asymptotic region to obtain $\mathbf{Y}(R_{\mathrm{asy}})$, where the interaction potential energy is sufficiently small compared with the collision energy. In Manolopoulos' improved LogD method, the propagation sector (a, b) is uniformly divided to two half-sectors, (a, c) and (c, b) with $c - a = b - c \equiv h$. In the following equations, the half sector (R', R'') denotes both (a, c) and (c, b) intervals. Here, we use the same matrix notations as Manolopoulos from Eqs. (38)–(43), which should not be confused with our matrix notations above. The propagator proceeds as

$$\mathbf{Y}(R'') = \mathrm{y}_4 - \mathrm{y}_3\big[\mathbf{Y}(R') + \mathrm{y}_1\big]^{-1}\mathrm{y}_2, \tag{38}$$

where

$$\begin{aligned} \mathrm{y}_1 &= y_1 + \mathbf{Q}(R'),\\ \mathrm{y}_2 &= y_2,\\ \mathrm{y}_3 &= y_3,\\ \mathrm{y}_4 &= y_4 + \mathbf{Q}(R''), \end{aligned} \tag{39}$$

and

$$(y_1)_{i,j} = (y_4)_{i,j} = \delta_{i,j}\begin{cases} |p_j|\coth(|p_j|h), p_j^2 \geq 0, \\ |p_j|\cot(|p_j|h), p_j^2 \leq 0, \end{cases}$$
$$(y_2)_{i,j} = (y_3)_{i,j} = \delta_{i,j}\begin{cases} |p_j|\mathrm{csch}(|p_j|h), p_j^2 \geq 0, \\ |p_j|\csc(|p_j|h), p_j^2 \leq 0. \end{cases} \quad (40)$$

For both half sectors, the **Q** matrices are

$$\mathbf{Q}(a) = \frac{h}{3}\mathbf{U}(a),$$
$$\mathbf{Q}(c) = \frac{4}{h}\left[\mathbf{I} - \frac{h^2}{6}\mathbf{U}(c)\right]^{-1} - \frac{4}{h}\mathbf{I}, \quad (41)$$
$$\mathbf{Q}(b) = \frac{h}{3}\mathbf{U}(b),$$

where

$$U_{i,j}(R) = W_{i,j}(R) - \delta_{i,j}p_j^2 \quad (42)$$

and

$$p_j^2 = W_{j,j}(c). \quad (43)$$

Note, despite that p_j is a complex number, all propagator matrix elements are real.

In ABC+D, we divide the propagation interval (R_0, R_{asy}) into three segments so that different propagation step lengths h can be used. For the short-range (small R) where potential energy varies rapidly with R, h should be small, while for the long-range, h can be relatively large. Using various h values rather than a uniform, one can reduce the number of propagation steps and computational cost.

The extraction of the S-matrix from $\mathbf{Y}(R_{\mathrm{asy}})$ is carried out as follows: First, a transformation of representation is performed from the DF frame (K-labeled) into SF one (L-labeled), which is discussed below. Then, the reaction matrix **K** is calculated by

$$\mathbf{K} = -\left[\mathbf{Y}(R_{\mathrm{asy}})\mathbf{N}(R_{\mathrm{asy}}) - \mathbf{N}'(R_{\mathrm{asy}})\right]^{-1}\left[\mathbf{Y}(R_{\mathrm{asy}})\mathbf{J}(R_{\mathrm{asy}}) - \mathbf{J}'(R_{\mathrm{asy}})\right]. \quad (44)$$

It can be divided into open–open, open–closed, closed–open, and closed–closed submatrices according to the internal energy of each channel,

$$\mathbf{K} = \begin{bmatrix} \mathbf{K}_{\mathrm{OO}} & \mathbf{K}_{\mathrm{OC}} \\ \mathbf{K}_{\mathrm{CO}} & \mathbf{K}_{\mathrm{CC}} \end{bmatrix}, \quad (45)$$

and the S-matrix only involves the open–open submatrix of **K**,

$$\mathbf{S} = (\mathbf{I} + \mathrm{i}\mathbf{K}_{\mathrm{OO}})^{-1}(\mathbf{I} - \mathrm{i}\mathbf{K}_{\mathrm{OO}}). \quad (46)$$

Here, **J** and **N** and their first-order derivatives **J**′ and **N**′ are diagonal matrices. For the open channels,

$$J_{i,j}(R) = \delta_{i,j}k_j^{-1/2}\tilde{j}_{L_j}(k_jR),$$
$$N_{i,j}(R) = \delta_{i,j}k_j^{-1/2}\tilde{n}_{L_j}(k_jR),$$
$$J'_{i,j}(R) = \delta_{i,j}k_j^{1/2}\tilde{j}'_{L_j}(k_jR), \quad (47)$$
$$N'_{i,j}(R) = \delta_{i,j}k_j^{1/2}\tilde{n}'_{L_j}(k_jR),$$

where $\tilde{j}_{L_j}$ and $\tilde{n}_{L_j}$ are Riccati–Bessel functions of the first and the second kinds, respectively, with their argument L_j being the orbital angular momentum of each channel. For closed channels, we have

$$J_{i,j}(R) = \delta_{i,j},$$
$$N_{i,j}(R) = \delta_{i,j},$$
$$J'_{i,j}(R) = \delta_{i,j}\left[\frac{1}{2R} + k_j\frac{I'_{L_j+1/2}(k_jR)}{I_{L_j+1/2}(k_jR)}\right], \quad (48)$$
$$N'_{i,j}(R) = \delta_{i,j}\left[\frac{1}{2R} + k_j\frac{K'_{L_j+1/2}(k_jR)}{K_{L_j+1/2}(k_jR)}\right],$$

where I and K are modified Bessel functions of the first and the third kinds, respectively. The Riccati–Bessel functions and the modified Bessel functions can be evaluated by Temme's excellent Algol routines[55,56] with positive real arguments and real orders.

Because the modified Bessel functions increase or decrease exponentially with respect to R and/or L_j, numerical difficulties may occur for large/small k_jR and large L_j values. Specifically, the values of I and K could exceed computer's capacity to store as double precision numbers. However, the values of I'/I and K'/K are rather small. In ABC+D, we add the asymptotic form of modified Bessel functions in case of double precision number overflow. For cases $k_jR \geq (L_j + 1/2)^2 - 1/4$,

$$J'_{i,j}(R) \cong \frac{1}{2R} + k_j,$$
$$N'_{i,j}(R) \cong \frac{1}{2R} - k_j; \quad (49)$$

and for cases $k_jR < L_j + 3/2$,

$$J'_{i,j}(R) \cong \frac{1 + 2k_j(L_j + 1/2)}{2R},$$
$$N'_{i,j}(R) \cong \frac{1 - 2k_j(L_j + 1/2)}{2R}. \quad (50)$$

To our best knowledge, Eqs. (49) and (50) have not been reported before.

F. Transformation of representation

After the propagation, one obtains the LogD matrix **Y** in the helicity representation or the DF frame, which needs to be transformed from the DF frame to the SF frame via an orthogonal matrix **B**,

$$|j_2tL;J\varepsilon\rangle = \sum_{K=0}^{K_m} B_{KL}^{Jj_2\varepsilon}|j_2tK;J\varepsilon\rangle. \quad (51)$$

If the basis sets are "complete", where $K_m = \min(J, j_2)$, then **B** is analytical as

$$B_{KL}^{Jj_2\varepsilon} = \sqrt{2 - \delta_{K,0}}\sqrt{\frac{2L+1}{2J+1}}\langle j_2KL0|JK\rangle. \quad (52)$$

The LogD matrix in the SF frame are calculated by

$$\mathbf{Y}^{\mathrm{SF}} = \mathbf{B}^{\mathrm{T}}\mathbf{Y}^{\mathrm{DF}}\mathbf{B}. \quad (53)$$

In ABC+D, we provide an option to use the so-called K-truncation scheme,[57] where a parameter $K_{\max}$ can be set to truncate the value of K as $K_m = \min(J, j_2, K_{\max})$, leading an "incomplete" basis set in the scattering calculation. If $K_{\max} \geq \min(J, j_{2,\max})$, this approximation recovers the exact TICC approach. Otherwise for $K_{\max} < \min(J, j_{2,\max})$, the matrix **B** is no longer analytical and L is no longer an integer. In ABC+D, by diagonalizing the centrifugal matrix **U**, which is the corresponding matrix of operator $\mathbf{L}^2$, we obtain the eigenvalues of $L(L+1) \equiv \ell$ as well as the eigenvectors as the orthogonal transformation matrix **B**. Thus, the eigenvalue of L is calculated by $L = \sqrt{\ell + 1/4} - 1/2$, and the negative root of L is dropped. We note that the "incomplete" helicity basis functions are also employed in the extended coupled-states approximation discussed below, where we thus use similar methodology by diagonalizing the **U** matrix to implement the transformation between DF and SF frames.

One can transform the S-matrix in SF frame back to the BF frame by

$$S_{K',K} = \sum_{L',L} \mathrm{i}^{L-L'} B_{K',L'} S_{L',L} B_{L,K} \tag{54}$$

in which other irrelevant subscripts are dropped. Finally, the state-to-state probability for elastic and inelastic transitions can be calculated in terms of the T-matrix,

$$P^J_{j'_2 t' \leftarrow j_2 t}(E_c) = \sum_{K' K \varepsilon} \left| T^{J\varepsilon}_{j'_2 t' K', j_2 t K}(E_c) \right|^2, \tag{55}$$

where the T-matrix is evaluated by $\mathbf{T} = \mathrm{I}\text{-}\mathbf{S}$.

G. Extended coupled-states approximation

In ABC+D, we provide an option to use the extended coupled-states (ECS) approximation for solving the non-reactive scattering problems,[35,58] which was an extended version of original coupled-states approximation.[59,60] In the ECS approximation, the entire matrix **W** in Eq. (34) is replaced by several K-labeled submatrices blocks, which only include a limited number of neighboring helicity (K', K) blocks (Coriolis couplings). The partition of matrices in the ECS approximation is rationalized by the weak Coriolis couplings between far away K blocks. Unlike the K-truncation approximation that neglects high K helicity channels completely, the ECS approximation retains all helicity states but with couplings to a few neighboring channels.

By defining the number of nearest K blocks included as Δ, the **U** matrix is now evaluated as

$$\begin{aligned} U^{J\varepsilon,\mathcal{K}}_{j'_2 t' K', j_2 t K} = \delta_{j'_2, j_2} \delta_{t', t} \Big\{ & \delta_{K',K} \left[J(J+1) + j_2(j_2+1) - 2K^2 \right] \\ & - \delta_{K',K+1} \sqrt{1 + \delta_{K0}} \lambda^+_{JK} \lambda^+_{j_2 K} \\ & - \delta_{K',K-1} \sqrt{1 + \delta_{K1}} \lambda^-_{JK} \lambda^-_{j_2 K} \Big\}, \end{aligned} \tag{56}$$

where $\mathcal{K} - \Delta \leq K \leq \mathcal{K} + \Delta$. Under such circumstances, the valid value range of $\mathcal{K}$ is $\Delta \leq \mathcal{K} \leq J - \Delta$. Note that **V** matrix retains its expression in Eq. (26) as in rigorous TICC because it is block diagonal in K. So in ECS, the CC equations with the full matrix is replaced by several CC equations with smaller $\mathcal{K}$-labeled submatrices, which yield $\mathcal{K}$-labeled S-matrices. Finally, the state-to-state probability is calculated as follows:

$$P^J_{j'_2 t' \leftarrow j_2 t}(E_c) = \sum_{\varepsilon} \sum_{K=0}^{J} \sum_{K'=\mathcal{K}-\Delta}^{\mathcal{K}+\Delta} \left| S^{J\varepsilon,\mathcal{K}}_{j'_2 t' K', j_2 t K}(E_c) \right|^2. \tag{57}$$

If $\Delta = 0$, this ECS approach recovers the original CS approximation, where no Coriolis coupling is included. If $\Delta \geq (J+1)/2$ for odd valued J (or $\Delta \geq J/2$ for even valued J), only one block $\mathcal{K} = (J+1)/2$ is needed and it is thus exactly equivalent to the rigorous TICC.

H. Linear algebra

In ABC+D, the matrix operations include matrix–matrix multiplication, matrix diagonalization, and matrix inversion. LAPACK routines[61] are used to perform these computational tasks.

Once a diagonalization is accomplished, the sign of each eigenvector needs be set up manually because the sign of the eigenvector is undetermined. In ABC+D, we stipulate the following criteria to assign a consistent sign for all eigenvectors. (i) In diagonalizing the 1D Hamiltonian to obtain eigenfunctions $\xi_{l_1 v_1}$ and $\zeta_{l_2 v_2}$, the sign is chosen to make sure the first peak of the wavefunction to be positive, and others are adjusted accordingly. (ii) The transformation matrix **T** is obtained by diagonalizing the monomer's Hamiltonian matrix. We set the first element of each eigenvector, $T^{j_2 K}_{\chi=1,t}$, to be positive, and others are adjusted accordingly. (iii) The orthogonal matrix **B** is obtained by diagonalizing **U**. The stipulation of its signs must fully conform to Eq. (52) in case of a "complete" basis set. To this end, the last element of each eigenvector and $(-1)^{j_2+K_m} B^{j_2}_{K_m L}$ is set to be positive and others are adjusted accordingly.

I. Coordinate transformation

In practice, the potential energy surface (PES) may be expressed in various coordinate systems. To obtain correct potential energy at each quadrature point in the BAST coordinates, coordinate transformations must be correctly performed. In ABC+D, we provide with one of such subroutines that transform the internal coordinates into Cartesian coordinates, for both the triatomic monomer and entire tetra-atomic system, from which the coordinates used in the PES can be readily obtained. The corresponding algorithm is briefly introduced here.

For the triatomic monomer, it is placed onto a two-dimensional plane with the vector $\vec{r}_1$ (a Radau bond length) lying along the Cartesian x-axis and its Radau canonical point being the origin O. So we can calculate the coordinates of atom A $(r_1, 0)$, C $(r_2 \cos\theta_1, r_2 \sin\theta_1)$ and its center of mass E. The coordinate of atom B is calculated according to the formula $\overrightarrow{\mathrm{OB}} = \overrightarrow{\mathrm{OE}}\left(1 - \sqrt{m_{\mathrm{ABC}}/m_{\mathrm{B}}}\right)$. Note that atom B is placed on the inverse direction of E with respect to the origin O.

The Cartesian coordinates in the DF frame of the ABC+D system are shown in Fig. 1. Atom D $(0, 0, R)$ is first calculated. Assume the ABC monomer is initially placed on the xOz plane, and their initial Cartesian coordinates are calculated as implemented for the triatomic system, denoted as A′ and C′. By rotating A′ along $\overrightarrow{\mathrm{OB}}$ with an angle of ϕ, the coordinate of A is obtained. For an arbitrary point (x', y', z'), the rotation along arbitrary unit vector (n_x, n_y, n_z) anticlockwise with θ is done by a transformation $(x, y, z) = (x', y', z')\mathbf{R}(\vec{n}, \theta)$, where

$$\mathbf{R}(\vec{n},\theta)=\begin{bmatrix} n_x^2(1-\cos\theta)+\cos\theta & n_xn_y(1-\cos\theta)+n_z\sin\theta & n_xn_z(1-\cos\theta)-n_y\sin\theta \\ n_xn_y(1-\cos\theta)-n_z\sin\theta & n_y^2(1-\cos\theta)+\cos\theta & n_yn_z(1-\cos\theta)+n_x\sin\theta \\ n_xn_z(1-\cos\theta)+n_y\sin\theta & n_yn_z(1-\cos\theta)-n_x\sin\theta & n_z^2(1-\cos\theta)+\cos\theta \end{bmatrix}. \quad (58)$$

Similar operations are implemented with C' to get C.

J. Summary of the program

The executive flow of the program is summarized in Fig. 2. Firstly, ABC+D reads parameters from an input file source.dat. Second, the primitive basis functions are prepared and the monomer Hamiltonians are diagonalized to obtain the transformation matrix **T**. Then, the contracted basis functions and matrices in the CC equations are prepared. ABC+D treats LogD matrices of multiple total energies simultaneously, by calling for an energy-independent interaction PEO matrix **V**. Namely, in the propagation process, $\mathbf{V}(R')$ is calculated for the current LogD step R', and it is repeatedly used to calculate all $\mathbf{Y}(R')$ matrices. Once $\mathbf{Y}(R')$ matrices of all energies are obtained, $\mathbf{V}(R'')$ is calculated and used for all $\mathbf{Y}(R'')$ matrices. Finally, after the propagation is finished, *S*-matrix elements at each total energy are extracted individually. The state-to-state integral cross section is calculated as

$$\sigma_{j_2't'\leftarrow j_2t}(E_c)=\frac{1}{2j_2+1}\frac{\pi}{2\mu E_c}\sum_J(2J+1)P^J_{j_2't'\leftarrow j_2t}(E_c). \quad (59)$$

The state-to-state differential cross section is calculated in terms of *T*-matrix elements as

$$\frac{d\sigma_{j_2't'\leftarrow j_2t}(\vartheta,E_c)}{d\Omega}=\frac{1}{2j_2+1}\sum_{K'K}\left|\frac{1}{2ik_{j_2t}}\sum_{J\varepsilon}(2J+1)d^J_{K',K}(\vartheta)T^{J\varepsilon}_{j_2't'K',j_2tK}(E_c)\right|^2, \quad (60)$$

where $d^J_{K',K}(\vartheta)$ is an element of the reduced rotational matrix with scattering angle ϑ.

To verify the new code, we have compared the rotationally inelastic cross sections using the current code with a previous calculation for the case of H_2O + He scattering, and the agreement is satisfactory.[39] This code was further applied to investigate the ro-vibrationally inelastic scattering for the H_2O + Cl[39] and H_2O + Ar systems.[58,62,63] More recently, the stereodynamics of the H_2O + He scattering was investigated with the *S*-matrix elements calculated using this code.[64]

III. A CALCULATION EXAMPLE

The H_2O + Cl system is chosen to illustrate how to run the ABC+D program. The Li–Dawes–Guo potential energy surface (PES)[65] is used for this tetra-atomic system, while the PES of Jiang *et al.*[66] is used for computing the ro-vibrational states of H_2O.

A. Distributed files and input parameters

The current version of ABC+D program contains two folders: ABC+D_Kmax and ABC+D_ECS, in which the *K*-truncation scheme and ECS approximation can be used for implementation. Same files are included in these two folders:

(1) the input file: source.dat; (different parameters are placed in this file for the two folders and are discussed in Table I)
(2) the Fortran code files for the scattering calculations: module.f, main.f, channel.f, matrix.f, pes_interface.f, function.f, propagation.f, match.f;
(3) a GNU makefile that can build the executable for the dynamical calculations: Makefile;
(4) PES related files: biases.txt, check-adi.txt, clh2o-pipnn.f, new8-final.dat, potent.f, weights.txt;

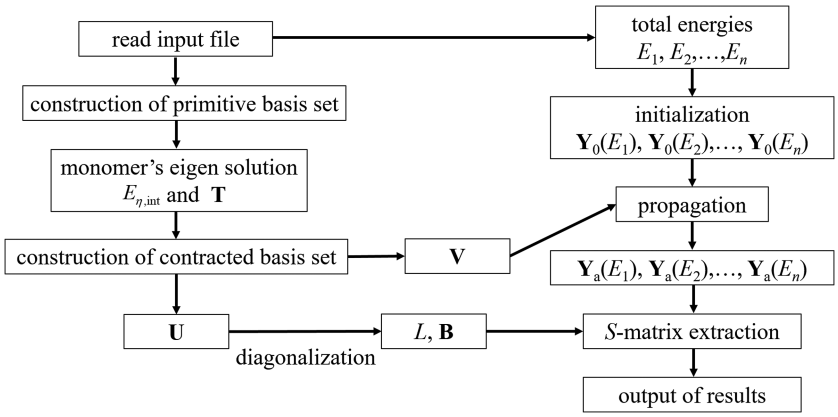

FIG. 2. Executive flow of the ABC+D program.

TABLE I. Input parameters for the test calculation on the H_2O + Cl system. Distance quantities are in Bohr, angles in degree, and energies in cm^{-1}.

Parameter	Explanation
	`module.f`
`m_A`, `m_B`, `m_C`, `m_D`	Masses of the four atoms in atomic mass units
`Ndvr1`, `Ndvr2`, `Nth1`	Number of DVR or quadrature points for primitive basis
`Np1`,`Np2`,`Nl3`,`Nl4`,`Nl5`	Number of PODVR or quadrature points for contracted basis
`r1_eq`, `r2_eq`, `th1_eq`	Equilibrium geometry of monomer in Radau coordinates
	`source.dat`
`x0_r1`, `xe_r1`, `x0_r2`, `xe_r2`	Intervals of DVR grids
`x0_RR`, `x1_RR`, `x2_RR`, `xe_RR`	Intervals of propagation grids along R
`h1`, `h2`, `h3`	Propagation step lengths of three segments
`eemax`	Contracted basis internal energy truncation
`v1max`, `v2max`, `j1max`	Maximum quantum numbers to truncate the primitive basis
`j2max`, `tmax`	Maximum quantum numbers to truncate the contracted basis
`Kmax`	Maximum value of quantum number K (this parameter only exists in folder `ABC+D_Kmax`)
`NNK`	Number of nearest K-blocked submatrices involved (Δ) (this parameter only exists in folder `ABC+D_ECS`)
`Jtot`, `ipar`, `jpar`	Total angular momentum J, system parity ε, exchange parity P_{ex} (for ABC-type monomers, set `jpar` = 0)
`nEtot`	Number of total energy points
`Etot`	Array of total energy points
`tot_thread`	The number of threads in OpenMP parallel process

(5) a plain-text file that allows customized choices of contracted basis set: `cbasis.txt`.

Before compiling, the input parameters are modified in `module.f` and `source.dat`, in which the namelist parameters of input data are shown in Table I. A practical limit for the number of contracted basis is a few thousand, due to the expensive matrix operations in the calculations. For a typical supercomputer with the capacity of ~100 GB virtual memory, a single run of calculation is able to deal with some hundreds total energies simultaneously, without a major excessive central processing unit (CPU) time cost than that of only one total energy involved.

ACKNOWLEDGMENTS

We acknowledge support from a MURI grant from ARO (Grant No. W911NF-19-1-0283 to H.G.). D.X. acknowledges the Innovation Program for Quantum Science and Technology (Grant No. 2021ZD0303305) and National Natural Science Foundation of China (Grant Nos. 22233003 and 22241302 to D.X.) for partial support. The calculations were performed at the Center for Advanced Research Computing (CARC) at the University of New Mexico.

AUTHOR DECLARATIONS

Conflict of Interest

The authors have no conflicts to disclose.

Author Contributions

Dongzheng Yang: Investigation (equal); Software (lead); Writing – original draft (equal). **Shijie Chai**: Investigation (equal); Software (supporting). **Daiqian Xie**: Resources (equal); Supervision (equal); Writing – review & editing (equal). **Hua Guo**: Resources (lead); Supervision (lead); Writing – review & editing (lead).

DATA AVAILABILITY

The data that support the findings of this study are openly available in (`ABC+D`) at http://dx.doi.org/10.17632/2svn4wjsr7.1.

REFERENCES

[1] R. D. Levine, *Molecular Reaction Dynamics* (Cambridge University Press, Cambridge, 2005).
[2] A. W. Jasper, J. Phys. Chem. A **124**, 1205–1226 (2020).
[3] E. Roueff and F. Lique, Chem. Rev. **113**, 8906–8938 (2013).
[4] J. R. Barker and D. M. Golden, Chem. Rev. **103**, 4577–4591 (2003).
[5] R. V. Krems, Phys. Chem. Chem. Phys. **10**, 4079–4092 (2008).
[6] S. Y. T. van de Meerakker, H. L. Bethlem, N. Vanhaecke, and G. Meijer, Chem. Rev. **112**, 4828–4878 (2012).
[7] E. Narevicius and M. G. Raizen, Chem. Rev. **112**, 4879–4889 (2012).
[8] G. Quéméner and P. S. Julienne, Chem. Rev. **112**, 4949–5011 (2012).
[9] B. K. Stuhl, M. T. Hummon, and J. Ye, Annu. Rev. Phys. Chem. **65**, 501–518 (2014).
[10] J. Jankunas and A. Osterwalder, Annu. Rev. Phys. Chem. **66**, 241–262 (2015).
[11] N. Balakrishnan, J. Chem. Phys. **145**, 150901 (2016).

[12]K. Takayangi, Adv. At. Mol. Phys. **1**, 149–194 (1965).
[13]J. M. Hutson, in *Cold Molecules: Theory, Experiment, Applications*, edited by R. V. Krems, W. C. Stwalley, and B. Friedrich (Taylor & Francis, London, 2009), pp. 3–37.
[14]J. M. Bowman and G. C. Schatz, Annu. Rev. Phys. Chem. **46**, 169–195 (1995).
[15]J. Z. H. Zhang, *Theory and Application of Quantum Molecular Dynamics* (World Scientific, Singapore, 1999).
[16]D. Skouteris, J. F. Castillo, and D. E. Manolopoulos, Comput. Phys. Commun. **133**, 128 (2000).
[17]W. Hu and G. C. Schatz, J. Chem. Phys. **125**, 132301 (2006).
[18]S. C. Althorpe and D. C. Clary, Annu. Rev. Phys. Chem. **54**, 493–529 (2003).
[19]H. Guo, Int. Rev. Phys. Chem. **31**, 1–68 (2012).
[20]D. H. Zhang and H. Guo, Annu. Rev. Phys. Chem. **67**, 135–158 (2016).
[21]B. Fu, X. Shan, D. H. Zhang, and D. C. Clary, Chem. Soc. Rev. **46**, 7625–7649 (2017).
[22]R. G. Newton, *Scattering Theory of Waves and Particles* (Springer-Verlag, New York, 1982).
[23]G. G. Balint-Kurti and A. P. Palov, *Theory of Molecular Collisions* (Royal Society of Chemistry, Cambridge, 2015).
[24]W. A. Lester, in *Dynamics of Molecular Collision*, edited by W. H. Miller (Plenum, New York, 1976).
[25]R. Kosloff, J. Phys. Chem. **92**, 2087–2100 (1988).
[26]R. Kosloff, Annu. Rev. Phys. Chem. **45**, 145 (1994).
[27]J. Z. H. Zhang, J. Dai, and W. Zhu, J. Phys. Chem. A **101**, 2746–2754 (1997).
[28]H. Guo, in *Theory of Chemical Reaction Dynamics*, edited by A. Lagana and G. Lendvay (Kluwer, Dordrecht, 2004), pp. 217–229.
[29]G. G. Balint-Kurti, Int. Rev. Phys. Chem. **27**, 507–539 (2008).
[30]B. Zhao and H. Guo, WIRES: Comput. Mol. Sci. **7**, e1301 (2017).
[31]J. M. Hutson and C. R. Le Sueur, Comput. Phys. Commun. **241**, 9–18 (2019).
[32]M. H. Alexander, D. E. Manolopoulos, H.-J. Werner, B. Follmeg, P. J. Dagdigian, P. F. Vohralik, D. Lemoine, G. Corey, R. Gordon, B. Johnson, T. Orlikowski, A. Berning, A. Degli-Esposti, C. Rist, B. Pouilly, G. v. d. Sanden, M. Yang, F. d. Weerd, S. Gregurick, J. Klos, and F. Lique, HIBRIDON, University of Marylang, 2011.
[33]J. Zuo and H. Guo, J. Chem. Phys. **153**, 144306 (2020).
[34]R. V. Krems, TwoBC, University of British Columbia, Vancouver, 2006.
[35]D. Yang, X. Hu, D. H. Zhang, and D. Xie, J. Chem. Phys. **148**, 084101 (2018).
[36]T. Stoecklin, L. D. Cabrera-González, O. Denis-Alpizar, and D. Páez-Hernández, J. Chem. Phys. **154**, 144307 (2021).
[37]L. D. Cabrera-González, O. Denis-Alpizar, D. Páez-Hernández, and T. Stoecklin, Mon. Not. R. Astron. Soc. **514**, 4426–4432 (2022).
[38]T. Selim, A. van der Avoird, and G. C. Groenenboom, J. Chem. Phys. **157**, 064105 (2022).
[39]D. Yang, D. Xie, and H. Guo, J. Phys. Chem. A **125**, 6864–6871 (2021).
[40]G. Brocks, A. van der Avoird, B. T. Sutcliffe, and J. Tennyson, Mol. Phys. **50**, 1025–1043 (1983).
[41]R. Radau, Ann. Sci. Ecole. Norm. Superior **5**, 311–375 (1868).
[42]X.-G. Wang and T. Carrington, J. Chem. Phys. **146**, 104105 (2017).
[43]B. R. Johnson, J. Comput. Phys. **13**, 445–449 (1973).
[44]D. E. Manolopoulos, J. Chem. Phys. **85**, 6425–6429 (1986).
[45]R. N. Zare, *Angular Momentum: Understanding Spatial Aspects in Chemistry and Physics* (Wiley, New York, 1988).
[46]D. T. Colbert and W. H. Miller, J. Chem. Phys. **96**, 1982 (1992).
[47]J. Echave and D. C. Clary, Chem. Phys. Lett. **190**, 225–230 (1992).
[48]H. Wei and T. Carrington, Jr., J. Chem. Phys. **97**, 3029–3037 (1992).
[49]D. C. Clary and J. P. Henshaw, Faraday Discuss. Chem. Soc. **84**, 333–349 (1987).
[50]E. J. Rackham, F. Huarte-Larranaga, and D. E. Manolopoulos, Chem. Phys. Lett. **343**, 356–364 (2001).
[51]E. J. Rackham, T. Gonzalez-Lezana, and D. E. Manolopoulos, J. Chem. Phys. **119**, 12895–12907 (2003).
[52]T. González-Lezana, Int. Rev. Phys. Chem. **26**, 29–91 (2007).
[53]D. Yang, J. Huang, X. Hu, D. Xie, and H. Guo, J. Chem. Phys. **152**, 241103 (2020).
[54]Y. Liu, M.-G. Hu, M. A. Nichols, D. Yang, D. Xie, H. Guo, and K.-K. Ni, Nature **593**, 379–384 (2021).
[55]W. H. Press, S. A. Teukolsky, W. T. Vetterling, and B. P. Flannery, *Numerical Recipes*, 2nd ed. (Cambridge University Press, Cambridge, 1992).
[56]N. M. Temme, J. Comput. Phys. **19**, 324–337 (1975).
[57]J. Z. H. Zhang, J. Chem. Phys. **94**, 6047–6054 (1991).
[58]D. Yang, D. Xie, and H. Guo, J. Chem. Phys. **157**, 164111 (2022).
[59]R. T. Pack, J. Chem. Phys. **60**, 633–639 (1974).
[60]P. McGuire and D. J. Kouri, J. Chem. Phys. **60**, 2488–2499 (1974).
[61]E. Anderson, Z. Bai, C. Bichof, J. Demmel, J. Dongarra, J. DuCroz, A. Greenbaum, S. Hammarling, A. McKenney, S. Ostrouchov, and D. Sorensen, *LAPACK Users' Guide* (SIAM, Philadelphia, 1995).
[62]D. Yang, L. Liu, D. Xie, and H. Guo, Phys. Chem. Chem. Phys. **24**, 13542–13549 (2022).
[63]L. Liu, D. Yang, H. Guo, and D. Xie, J. Phys. Chem. A **127**, 195 (2023).
[64]D. Yang, D. Xie, and H. Guo, J. Phys. Chem. Lett. **13**, 1777–1784 (2022).
[65]J. Li, R. Dawes, and H. Guo, J. Chem. Phys. **139**, 074302 (2013).
[66]B. Jiang, D. Xie, and H. Guo, J. Chem. Phys. **136**, 034302 (2012).